

The relatively young, metal-poor and distant open cluster NGC 2324

A. E. Piatti¹, J. J. Clariá², and A. V. Ahumada²

¹ Instituto de Astronomía y Física del Espacio, CC 67, Suc. 28, 1428 Buenos Aires, Argentina

² Observatorio Astronómico, Universidad Nacional de Córdoba, Laprida 854, 5000 Córdoba, Argentina
e-mail: claria@mail.oac.uncor.edu; andrea@mail.oac.uncor.edu

Received 12 January 2004 / Accepted 21 January 2004

Abstract. We have obtained CCD photometry in the Johnson V , Kron-Cousins I and CT_1 Washington systems for NGC 2324, a rich open cluster located $\sim 35^\circ$ from the Galactic anticentre direction. We measured V magnitudes and $V - I$ colours for 2865 stars and T_1 magnitudes and $C - T_1$ colours for 1815 stars in an area of 13.6×13.6 . The comparison of the cluster colour-magnitude diagrams with isochrones of the Geneva group yield $E(V - I) = 0.33 \pm 0.07$ and $V - M_V = 13.70 \pm 0.15$ for $\log t = 8.65$ ($t = 440$ Myr) and $Z = 0.008$ ($[\text{Fe}/\text{H}] = -0.40$), and $E(C - T_1) = 0.40 \pm 0.10$ and $T_1 - M_{T_1} = 13.65 \pm 0.15$ for the same age and metallicity level. The resulting $E(V - I)$ reddening value implies $E(B - V) = 0.25 \pm 0.05$ and a distance from the Sun of (3.8 ± 0.5) kpc. Star counts carried out within and outside the cluster region allowed us to estimate the cluster angular radius as 5.3 ± 0.3 (5.9 pc). When using the $E(B - V)$ reddening value here derived and the original Washington photometric data of Geisler et al. (1991) for the stars confirmed as red cluster giants from Coravel radial velocities, we found $[\text{Fe}/\text{H}] = -0.31 \pm 0.04$, which is in good agreement with the best fits of isochrones. Therefore, NGC 2324 is found to be a relatively young, metal-poor and distant open cluster located beyond the Perseus spiral arm. A comparison of NGC 2324 with 10 well-known open clusters of nearly the same age shows that the cluster metal abundance and its position in the Galaxy are consistent with the existence of a radial abundance gradient of -0.07 dex kpc^{-1} in the Galactic disc.

Key words. Galaxy: open clusters and associations: individual: NGC 2324 – Galaxy: general – techniques: photometric

1. Introduction

Open clusters have always played a prominent role in the delineation of the chemical as well as the dynamical evolution of the Galactic disc, while the individual stars they include constrain the formation and evolution of stars of varying mass. Open clusters provide unique information on the metallicities and gradients in the Galactic disc (e.g., Piatti et al. 1995; Chen et al. 2003), on the average stellar ages and radial velocities at different Galactic radii (e.g., Janes & Phelps 1994; Friel et al. 2002), on the relationship between age and metallicity (e.g., Strobel 1991; Friel 1995) and on the detailed morphology of the red giant region in the colour-magnitude diagram (e.g., Clariá et al. 1999; Mermilliod et al. 2001). Research work focused on any of the above mentioned topics require high-quality data about the greatest possible number of clusters having a wide age range.

The present paper belongs to a series devoted to some poorly studied open clusters, located in different Galactic radii, for which we measure in a homogeneous way distance, age, reddening and metallicity, using high-quality CCD photometry in the Johnson V , Kron-Cousins I and CT_1 Washington

systems. We have already reported results on the relatively young and metal-poor open cluster NGC 2194 (Piatti et al. 2003a, hereafter Paper I), on the intermediate-age cluster NGC 2627 (Piatti et al. 2003b) and on the old, metal-poor anticentre cluster Trumpler 5 (Piatti et al. 2004). The cluster of current interest is NGC 2324 (IAU designation C0701+011), also known as Cr 125 (Collinder 1931). As in the case of the above mentioned clusters, the present work has been carried out by using CCD VI_{KC} and CT_1 photometry.

NGC 2324 is located $\sim 35^\circ$ from the Galactic anticentre direction in a rich star field in Monoceros at equatorial coordinates $\alpha = 7^{\text{h}} 04^{\text{m}} 2$, $\delta = +01^\circ 04'$ (2000) and Galactic coordinates $l = 213.44$ and $b = +03.32$. This is a rich, intermediate- brightness, detached open cluster of Trumpler class II2r (Ruprecht 1966). NGC 2324 was first observed photographically by Cuffey (1941), who highlighted the relatively low reddening to this cluster, despite its very small Galactic latitude. This object was later studied photographically by Becker (1960), Hoag et al. (1961), Barkhatova (1963), Rahim & Hassan (1967) and Becker et al. (1976). As it was first noted by Cuffey (1941), all these studies yield relatively low $E(B - V)$ reddening values, typically lower than 0.11. In their catalogue of Galactic star clusters observed in three colours,

Send offprint requests to: A. E. Piatti, e-mail: andres@iafe.uba.ar

Becker & Fenkart (1971) give $d = 2270$ pc and $E(B - V) = 0.06$ for NGC 2324. Old distance determinations range from 0.5 kpc to 9.1 kpc (Alter et al. 1970), although most recent evidence places NGC 2324 between 3.2 and 4.2 kpc from the Sun. Phelps et al. (1994) defined the morphological age index δV as the magnitude difference between the main sequence turnoff and the clump in the $(V, V - I)$ colour-magnitude diagram, deriving $\delta V = 0.3$ for NGC 2324. This value implies an age of 800 Myr (Janes & Phelps 1994), rendering the cluster older than the Hyades. Janes & Phelps (1994) also derived a significantly larger reddening value of $E(B - V) = 0.28$ and a distance from the Sun of 3.18 kpc. More recently, Loktin et al. (2001) published a second version of their Open Cluster Catalogue (Loktin & Matkin 1994) reviewing the fundamental parameters of 423 clusters. Their updated distances are now based on a Hyades distance modulus of 3.27, this value being 0.06 mag smaller than that found from Hipparcos parallaxes, namely $(m - M_V) = 3.33 \pm 0.01$ (Perryman et al. 1998). By using the original data from Hoag et al. (1961) and Becker et al. (1976), Loktin et al. (2001) determined the following parameters for NGC 2324: $d = 3805$ pc, $E(B - V) = 0.127$ and 426 Myr. Dutra & Bica (2000) derived a far-infrared reddening $E(B - V)_{\text{FIR}} = 0.29$ for NGC 2324 from DIRBE/IRAS 100 μm -dust emission in the cluster field. Even though this far-infrared reddening agrees well with that derived by Janes & Phelps (1994), the aforementioned works prove that there is no agreement on the parameters for NGC 2324, as derived by various studies.

NGC 2324 has a relatively small angular diameter of about $8'$ (Lyngå 1987). Even when this feature renders it appropriate for CCD camera analysis, the only CCD photometric study up to date was performed by Kyeong et al. (2001), who obtained *UBVI* photometry within a field of about $20' \times 20'$. Their cluster colour-magnitude diagrams (CMDs) reveal a main sequence that reaches some 4 mag below the turnoff, a well-populated giant branch and a clump of stars near $V = 13.45$, $B - V = 1.05$ and $V - I = 1.18$. From the analysis of their CCD data they derived: $E(B - V) = 0.17 \pm 0.12$, while using the zero age main sequence and theoretical isochrones computed by Bertelli et al. (1994), they estimated a distance $d = 4.2$ kpc, a metallicity $[\text{Fe}/\text{H}] = -0.32$, and an age of 630 Myr.

NGC 2324 is particularly interesting for the number of red giant candidates it contains as well as for the multiple possibilities they provide in terms of cluster metal content derivation. Janes (1979) found $[\text{Fe}/\text{H}] = -0.39 \pm 0.37$ from ultraviolet excesses $\delta(U - B)$ of 13 assumed cluster giants. Geisler et al. (1992) derived a completely unexpected value of $[\text{Fe}/\text{H}] = -1.01 \pm 0.27$ from Washington photometry of 9 red giants. Gratton (2000) independently reduced the various photometric and spectroscopic sources into a homogeneous catalogue of $[\text{Fe}/\text{H}]$ abundances, reporting $[\text{Fe}/\text{H}] = -0.52$ for NGC 2324. More recently, Mermilliod et al. (2001) obtained very accurate Coravel radial velocities and *UBV* photoelectric photometry of 17 red giant candidates in the cluster field. These data allowed them to unambiguously confirm the membership status of 8 stars, 3 of which are spectroscopic binaries. Using only the red giant data and the isochrone fitting procedure they derived an apparent distance modulus $V - M_V = 12.95$, a very

small reddening value $E(B - V) = 0.02$ and an age of 800 Myr, assuming that the cluster has nearly solar metal content ($Z = 0.019$). On the other hand, using moderate-resolution spectroscopic data of 7 red giants, Friel et al. (2002) obtained individual radial velocities and a mean cluster metallicity of $[\text{Fe}/\text{H}] = -0.15 \pm 0.16$. Friel et al. (2002) determined radial velocities with errors larger than those obtained from the Coravel data. This is the reason why they included in their metallicity determination stars with radial velocities similar to the mean cluster value (within the errors), but with quite different metallicities.

Therefore, there are several reasons for a renewed study of this cluster. Firstly, the reddening values determined in previous studies range from 0.02 (Mermilliod et al. 2001) to about 0.29 (Dutra & Bica 2000), while the distances obtained by different authors vary from 2.3 kpc (Becker & Fenkart 1971) to 4.2 kpc (Kyeong et al. 2001). Secondly, different metallicity determinations yield very discrepant $[\text{Fe}/\text{H}]$ values ranging from $[\text{Fe}/\text{H}] \approx 0.0$ (Mermilliod et al. 2001) to $[\text{Fe}/\text{H}] = -1.01$ (Geisler et al. 1992). Finally, there does not seem to be a clear agreement either between the ages estimated in previous works. So NGC 2324 may be nearly as old as the Hyades (Kyeong et al. 2001) or even a 50 per cent older (Friel et al. 2002). We strongly support the view that the existing discrepancy in the determination of the basic cluster parameters warrants their re-determination, on the basis of more reliable data.

In the present study, we report the results obtained from CCD V_{KC} photometry up to $V \sim 20.0$ mag and CCD photometry in the *C* and T_1 bands of the Washington system up to $T_1 \sim 18.5$ mag in the cluster field. These data are used to make a new and independent determination of reddening, distance, age and metallicity. In Sect. 2 we briefly describe the observational material. In Sect. 3 we present the analysis of the photometric data, while in Sect. 4 we determine the main cluster parameters. In Sect. 5 the resulting basic properties for NGC 2324 are discussed in the framework of the structure and evolution of the Galactic disc, together with those of 10 well-known open clusters of nearly the same age as NGC 2324. Section 6 summarizes our main conclusions.

2. Observations and reductions

CCD photometry for the open cluster NGC 2324 was obtained during a five night observing run using the 0.9-m telescope and the 2048×2048 Tektronix 2K #3 CCD at the Cerro Tololo Inter-American Observatory (CTIO), Chile, on 1997 December 23–24. CCD images of the cluster area were obtained with the Johnson *V*, Kron-Cousins *I* and Washington *C* and T_1 filters (Canterna 1976). The observations were carried out as described in Paper I for the open cluster NGC 2194. The scale on the chip is $0''.40 \text{ pixel}^{-1}$ yielding an area of $13''.6 \times 13''.6$. The CCD was controlled by the CTIO ARCON 3.3 data acquisition system in the standard quad amplifier mode. The gain and readout noise are $5 \text{ e}^-/\text{ADU}$ and 4 e^- , respectively. We obtained one 20-s and two 10-s *V* exposures, two 5-s and one 10-s *I* exposures, two 30-s *C* exposures and two 5-s T_1 exposures for NGC 2324. The seeing was typically $1''.5$ during the observing night.

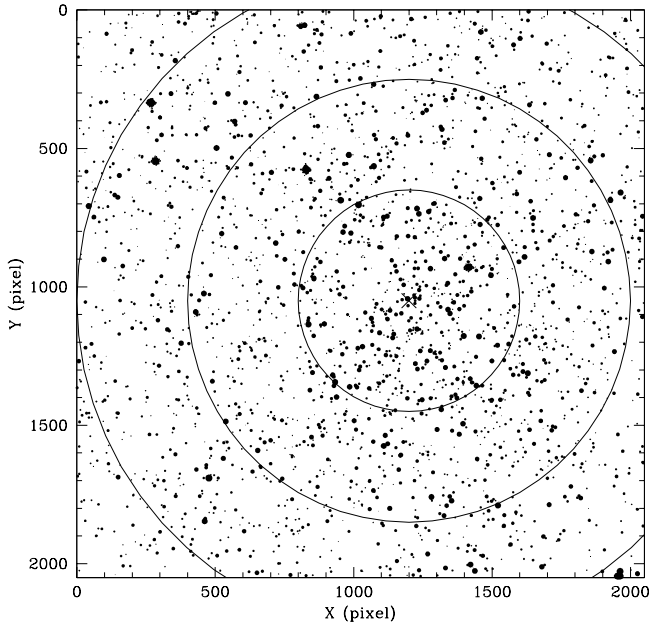


Fig. 1. Schematic finding chart of the stars observed in the field of NGC 2324. North is up and East is to the left. The sizes of the plotting symbols are proportional to the V brightness of the stars. Three concentric circles of 400, 800 and 1200 pixels wide around the cluster centre (*cross*) are also drawn.

Table 1. CCD VI data of stars in the field of NGC 2324.

Star	X (pixel)	Y (pixel)	V (mag)	$\sigma(V)$ (mag)	$V - I$ (mag)	$\sigma(V - I)$ (mag)	n
309	984.239	253.255	16.790	0.009	1.045	0.020	3
310	444.727	253.779	17.499	0.015	1.158	0.020	3
311	617.592	254.117	17.699	0.011	0.924	0.055	3
312	708.392	255.424	18.077	0.031	0.872	0.046	3
313	1142.572	256.372	18.061	0.011	0.983	0.050	3
.
.
.

NOTE: (X , Y) coordinates correspond to the reference system of Fig. 1. Magnitude and colour errors are the standard deviations of the mean, or the observed photometric errors for stars with one measurement.

Figure 1 shows a schematic finding chart of the cluster area built with all measured stars in the V -band. As in Paper I, we calibrated the observations in the VI_{KC} and Washington systems by means of the observation of numerous standard stars from the lists of Landolt (1992) and Geisler (1996). The data were reduced at the Instituto de Astronomía y Física del Espacio (Buenos Aires, Argentina) with stand-alone version of DAOPHOT II (Stetson 1987), after trimming, bias subtraction, and flat-fielding. Further details on the reduction and calibration methods are supplied in Paper I.

Table 1 gives in succession a running star number of the observed stars, X and Y coordinates in pixels (Fig. 1), V magnitudes and $V - I$ colours, along with the corresponding observational errors $\sigma(V)$ and $\sigma(V - I)$ and the number of

Table 2. CCD CT_1 data of stars in the field of NGC 2324.

Star	X (pixel)	Y (pixel)	T_1 (mag)	$\sigma(T_1)$ (mag)	$C - T_1$ (mag)	$\sigma(C - T_1)$ (mag)	n
504	1092.721	606.557	15.289	0.041	0.444	0.055	2
505	355.151	606.785	17.545	0.017	2.053	0.102	2
506	911.616	608.781	13.975	0.004	0.731	0.009	2
507	1480.182	610.937	17.352	0.021	1.296	0.010	2
508	844.170	611.209	15.450	0.012	1.444	0.037	2
.
.
.

NOTE: (X , Y) coordinates correspond to the reference system of Fig. 1. Magnitude and colour errors are the standard deviations of the mean, or the observed photometric errors for stars with one measurement.

Table 3. Magnitude and colour photometric errors as a function of V .

ΔV (mag)	σV (mag)	$\sigma(V - I)$ (mag)	σT_1 (mag)	$\sigma(C - T_1)$ (mag)
12–13	0.004	0.012	0.010	0.010
13–14	0.005	0.013	0.011	0.013
14–15	0.006	0.015	0.012	0.020
15–16	0.008	0.018	0.020	0.021
16–17	0.013	0.025	0.050	0.055
17–18	0.019	0.040	0.100	0.100
18–19	0.035	0.075	0.240	0.290
19–20	0.075	0.130	–	–
20–21	0.150	0.250	–	–

observations. The construction of this table is explained in Paper I. Table 2 provides the same information as for the C , T_1 photometry. Portions of Tables 1 and 2 are shown here for guidance regarding their form and content. Full display of these tables are available in electronic form at the CDS via anonymous ftp to cdsarc.u-strasbg.fr (130.79.128.5) or via <http://cdsweb.u-strasbg.fr/cgi-bin/qcat?J/A+A/418/979>. Table 3 shows how the V and T_1 magnitude and $V - I$ and $C - T_1$ colour errors (mean values) vary as a function of V for NGC 2324. Many of the stars observed at CTIO in the VI_{KC} system were also measured by Kyeong et al. (2001) and they show in general good agreement with the present observations. In fact, the mean differences and standard deviations are: $\Delta(V_{\text{our}} - V_{\text{kbs}}) = -0.011 \pm 0.038$ and $\Delta[(V - I)_{\text{our}} - (V - I)_{\text{kbs}}] = 0.030 \pm 0.070$, for 1570 and 1664 stars measured in common, respectively.

3. The (V , $V - I$) and (T_1 , $C - T_1$) colour–magnitude diagrams

The resulting VI photometry for all the stars measured in the field of NGC 2324 is shown in the CMD of Fig. 2. The cluster main sequence (MS) is easily identifiable, extending along ~ 7 mag and with clear evidence of some evolution. This suggests that the age of the cluster is some hundred million years

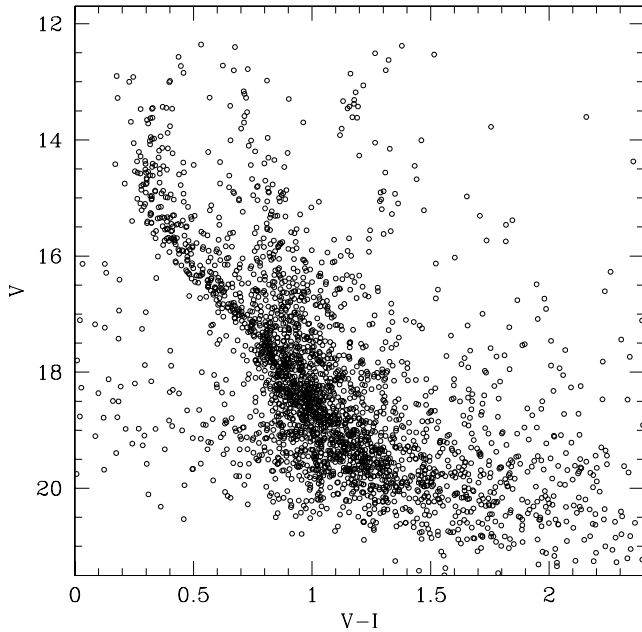


Fig. 2. $(V, V - I)$ colour-magnitude diagram for stars observed in the field of NGC 2324.

old. Outer Galactic disc stars remarkably contaminate the cluster MS, particularly its fainter half portion. Most of those field stars are grouped in a slightly tilted sequence roughly centred at $V - I = 0.9$ mag and extending from $V \sim 16$ down to 20 mag. At any rate, although this sequence overlaps the cluster MS, the position and shape of the latter is still distinguishable. If we continue in magnitude upwards from the broad field star sequence, younger field MS stars are also visible along a nearly vertical sequence with some colour dispersion. The figure also shows a clear red giant clump (RGC) at $(V, V - I) \approx (13.3, 1.15)$. The differences in magnitude and colour between the RGC and the MS turn-off also suggest that NGC 2324 is slightly younger than the Hyades.

We first examined the quality of our photometry in order to evaluate the influence of the photometric errors on the cluster fiducial characteristics of the CMD. From this inspection we found that 57 per cent of the total number of measured stars have three measures of their V magnitudes and $V - I$ colours and expand approximately from the brightest limit down to $V = 19.5$, while 15 and 28 per cent of the measured stars have two and one measures and cover V ranges from 18 to 20 mag and from 19 until the photometric limit, respectively. According to this crude statistics, the cluster MS is mainly defined by stars with three measures and the corresponding errors as shown in Table 3, i.e., $\sigma_V \leq 0.12$ mag for $V = 20$, $\sigma_V \leq 0.01$ mag for $12 < V < 16$, $\sigma_{V-I} \leq 0.12$ mag for $V = 19$ and $\sigma_{V-I} < 0.02$ mag for $V \leq 16$. Thus, the scatter produced by photometric errors is negligible in comparison with the colour width of the cluster MS.

We then examined the level of the field star contamination mentioned above by comparing the cluster CMD with the one corresponding to the field. In order to do that, we determined the cluster centre and its extension, and then built different CMDs with stars distributed in the cluster and field regions. To determine the position of the cluster centre we constructed

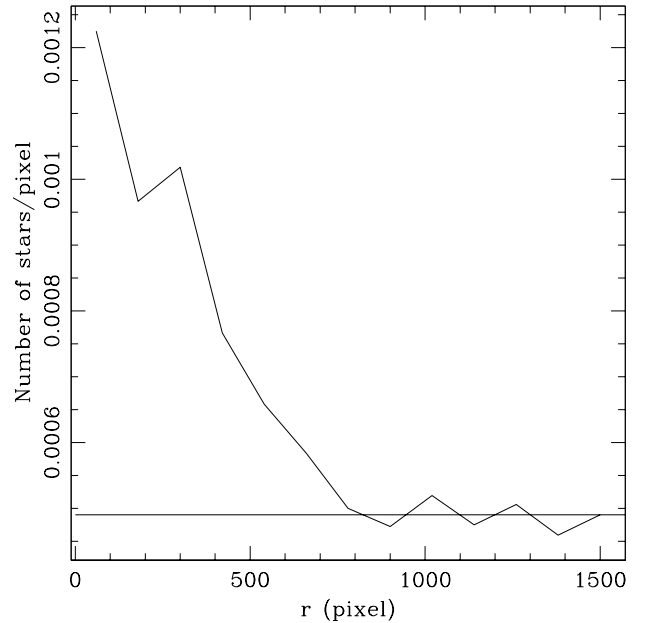


Fig. 3. Stellar density profile centred at $(X_C, Y_C) = (1200, 1050)$ pixels for stars observed in the field of NGC 2324.

projected stellar density profiles by counting the number of stars distributed in consecutive intervals along the X and Y axes. We then chose different size intervals with the aim of monitoring the evolution of the star count noise originated by stellar density fluctuations. We built five different sets of projected density profiles for bins with sizes between 100 and 150 pixels. For each pair of X and Y projected stellar density profiles, we fitted Gaussian functions to obtain the value of the cluster centre. During the fits we took care of spurious peaks caused by small concentrations of stars spread through the field. We averaged the five derived centres and adopted as the cluster centre the position $(X_C, Y_C) = (1200 \pm 50, 1050 \pm 50)$ pixels. This value is in very good agreement with the cluster centre spotted by eye when looking at the cluster finding chart.

Then, we estimated the cluster angular radius to delimit the extent of NGC 2324 over the observed area. Instead of counting stars lying in concentric rings as it is usually done, we preferred to carry out star counts in boxes of 120 pixels a side to facilitate adequate sampling of the star distribution normalized to the unit area as far as the boundary of the observed field. Alternatively, had we used concentric rings, the measure of the star density close to the corner of the observed field would have been more difficult to undertake. Thus, the number of stars per pixel for a given radius r was obtained by adding up stars counted in those boxes that lie within a ring Δr centred at r , divided by the area of the boxes considered in that sum. The radial profile obtained by using this procedure is shown in Fig. 3, which was built for $\Delta r = 120$ pixels. We did not find any difference when making the figure using a different Δr value between 100 and 150 pixels. From Fig. 3 we adopted the value $r_C = 800 \pm 50$ pixels, equivalent to 5.3 ± 0.3 , as the angular radius of the cluster. The two smaller rings drawn in Fig. 1 correspond to the full width at half maximum of the cluster stellar density ($r = 400$ pixels) and to the cluster radius, respectively.

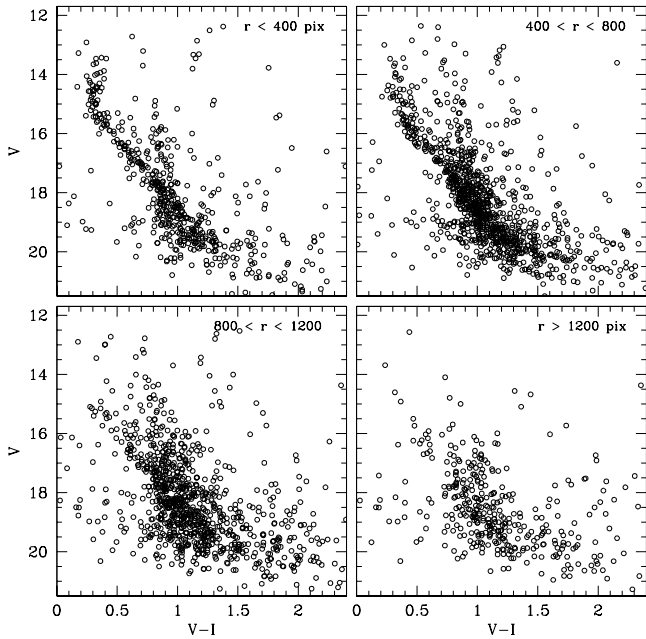


Fig. 4. $(V, V - I)$ colour–magnitude diagrams for stars observed in different extracted regions as indicated in each panel. See Sect. 3 for details.

Based on the above results, we built Fig. 4 with four CMDs extracted from three circular regions centred on the cluster. The extracted regions are labelled at the top of each panel. The upper left-hand panel clearly shows the cluster fiducial MS and the RGC, whereas in the lower right-hand panel the cluster features are practically absent. The upper right-hand panel appears dominated by cluster MS stars and the lower left-hand panel by field stars. Both CMDs provide detailed information about the cluster–field transition region. While the upper right-hand CMD insinuates an emerging relatively broad field star sequence superimposed onto the cluster MS, the lower left-hand panel reveals the existence of a composite field CMD dominated by intermediate-age and young disc stars. The emerging field sequence is also detected as an abrupt increase at $V \sim 17$ when tracing the luminosity function of the cluster MS. The fact that field star and cluster sequences appear overlapping suggests that both are affected by nearly the same interstellar reddening.

The different field features identified in the lower left-hand panel are not recognized in the $r > 1200$ pixels CMD at all, as should be expected if the field had a relatively homogeneous stellar composition. For example, field stars brighter than $V = 16.5$ are mainly seen in the CMD of the lower left-hand panel. This suggests that the field stellar composition varies across the observed sky area. For this reason, instead of carrying out a statistical field subtraction to the $r < 800$ pixels CMD using the $r > 1200$ pixels CMD as reference, we decided to use the innermost extracted CMD as representative of the cluster CMD and hence, to estimate its fundamental parameters. In addition, and in order to obtain a better definition of the cluster RGC, we combined the $r < 400$ pixels CMD with all the stars observed with $V < 14$ and $V - I > 1.0$.

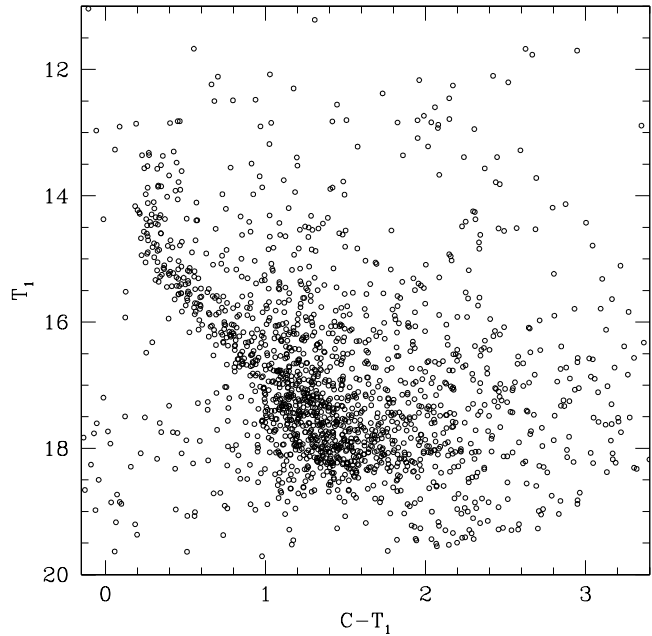


Fig. 5. $(T_1, C - T_1)$ colour–magnitude diagram for stars observed in the field of NGC 2324.

The resulting CMD with all the measured stars in the CT_1 Washington system is shown in Fig. 5. It contains approximately 40 per cent fewer stars than Fig. 2, because of the relatively brighter limiting magnitude reached with the Washington C -passband. For this reason, we based our choice of the parameters involved in the CMDs analysis (e.g., cluster centre, circular extractions, field area) on the VI photometry, rather than on the CT_1 one. The smaller number of measured stars did not preclude the CT_1 photometry from showing the same features as the VI data. Indeed, the cluster MS and the RGC are clearly recognizable, as well as the pattern of the contamination by the field stars. Moreover, all these features are displayed within a $C - T_1$ range approximately twice as wide as that for the $V - I$ colour. In order to account for the field contamination in the cluster CMD, we followed the same procedure applied to the VI data, and plotted the circular extracted CMDs in Fig. 6. The radii for the distinct extracted CMDs are labelled at the top of each panel. As can be seen, the same conclusions about the cluster features inferred from the VI data can also be drawn from Fig. 6. We used the $r < 400$ pixels CMD to estimate the physical properties of NGC 2324.

4. Fundamental properties of NGC 2324

We made use of the availability of theoretical isochrones recently computed for both VI and CT_1 photometric systems to estimate the reddening, distance, age and metallicity of NGC 2324. Particularly, we used those isochrones calculated with core overshooting effect by Lejeune & Schaerer (2001). On the other hand, since Geisler et al. (1992) and Friel et al. (2002) derived very deficient ($[Fe/H] = -1.01$) and slightly deficient ($[Fe/H] = -0.15$) metal abundances for the cluster, we initially decided to use chemical compositions of $Z = 0.02$, 0.008 and 0.004 for the isochrone sets. Firstly, we fitted the

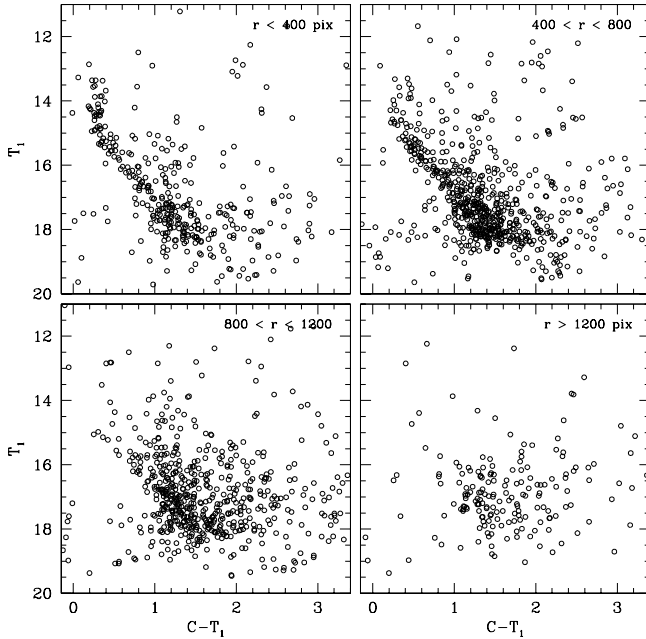


Fig. 6. $(T_1, C - T_1)$ colour-magnitude diagrams for stars observed in different extracted regions as indicated in each panel. See Sect. 3 for details.

zero age main sequence (ZAMS) of Lejeune & Schaerer (2001) to the $(V, V - I)$ CMD for each selected metallicity and derived the cluster colour excess $E(V - I)$ and the apparent distance modulus $V - M_V$. The relatively long observed cluster MS allowed for these parameters to be determined with accuracy. Secondly, we selected isochrones of ages of some hundred million years and younger than the Hyades, and used the three derived pairs of $(V - M_V, E(V - I))$ values to estimate the cluster age. Finally, we compared the best fits obtained from the three different metallicities and chose that which best resembles the upper MS, particularly the turn-off region, and the locus of the RGC. The isochrone of $\log t = 8.65$ ($t = 440$ Myr) and $Z = 0.008$ turned out to be the one which most properly reproduces the cluster features in the $(V, V - I)$ CMD. Note that $Z = 0.008$ implies $[\text{Fe}/\text{H}] = -0.40$, if Eq. (11) of Bertelli et al. (1994) is used. To match this isochrone, we used an $E(V - I)$ colour excess and a $V - M_V$ apparent distance modulus of 0.33 and 13.70 respectively, which were derived from the fit of the ZAMS for a metallicity level of $Z = 0.008$. The uncertainties of these parameters were estimated from the individual values obtained from the cluster feature dispersion. Thus, we estimated $\sigma(E(V - I)) = 0.07$ mag, $\sigma(V - M_V) = 0.15$ mag, and $\sigma(t) = {}^{+90}_{-40}$ Myr.

By employing the most frequently used values of 1.33 and 3.2 for the $E(V - I)/E(B - V)$ and $A_V/E(B - V)$ ratios, respectively, we obtained an $E(B - V)$ reddening value of 0.25 ± 0.05 and a distance from the Sun of (3.8 ± 0.5) kpc. Figure 7 shows the isochrone of $\log t = 8.65$ and $Z = 0.008$ (solid line), and two additional isochrones of 8.60 and 8.70 and $Z = 0.008$ (dotted and short-dashed lines, respectively) illustrating the fitting procedure. We also included the ZAMS corresponding to the same metal abundance level and marked with open circles the red giant members confirmed

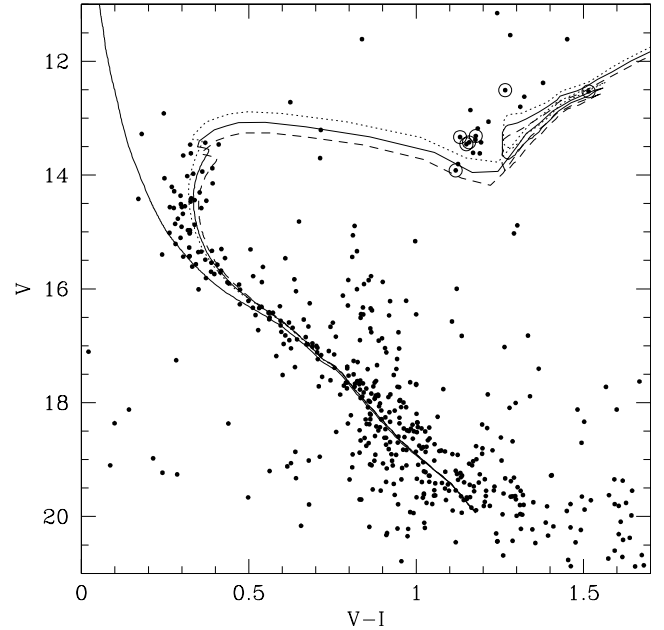


Fig. 7. $(V, V - I)$ colour-magnitude diagram for stars in NGC 2324. Isochrones from Lejeune & Schaerer (2001) of $\log t = 8.60$, 8.65 and 8.70, computed taking into account overshooting, are overplotted with dotted, solid and short-dashed lines, respectively.

by Mermilliod et al. (2001) from CORAVEL radial velocity observations. The RGC is the worst fitted feature by the theoretical isochrones. The loop in the isochrones corresponding to the bluest stage during the He-burning core phase is shifted redwards by about $\Delta(V - I) = 0.15$ mag with respect to the observed position of the cluster RGC. Theoretical RGCs have also frequently proved to be redder than the observed RGCs in previous studies of star clusters spanning ages from 0.3 up to 2.3 Gyr (see, e.g., Clariá et al. 1994; Geisler et al. 2003; Piatti et al. 2003a), although some other studies have found good agreement between theory and observations for RGCs of intermediate-age clusters (see, e.g., Clariá et al. 1999; Mermilliod et al. 2001). In particular, Piatti et al. (1998) confirmed the existence of a shift between the observed loops and the theoretically predicted ones for clusters older than 200 Myr from the comparison of empirical and Padova isochrones.

We followed the same steps as described above to estimate the cluster fundamental parameters from the $(T_1, C - T_1)$ CMD. We also used the ZAMS and sets of theoretical isochrones computed by Lejeune & Schaerer (2001) for three different metallicities ($Z = 0.02, 0.008$, and 0.004). We found that the isochrone of $\log t = 8.65$ and $Z = 0.008$ is unmistakably the best representative of the cluster features. For the fit we used $E(C - T_1) = 0.40$ and $T_1 - M_{T_1} = 13.65$, as derived from the ZAMS for a metal abundance of $[\text{Fe}/\text{H}] = -0.40$. Let us recall that the $C - T_1$ colour is a very sensitive metallicity indicator (Geisler et al. 1991), and consequently, isochrones for different Z values appear clearly separated in the $(T_1, C - T_1)$ CMD. The estimated errors for the cluster parameters are now: $\sigma(E(C - T_1)) = 0.10$ mag, $\sigma(T_1 - M_{T_1}) = 0.15$ mag, and $\sigma(t) = {}^{+90}_{-40}$ Myr. Similarly, by using $E(C - T_1)/E(B - V) = 1.97$ and $A_{T_1}/E(B - V) = 2.62$ (Geisler et al. 1996),

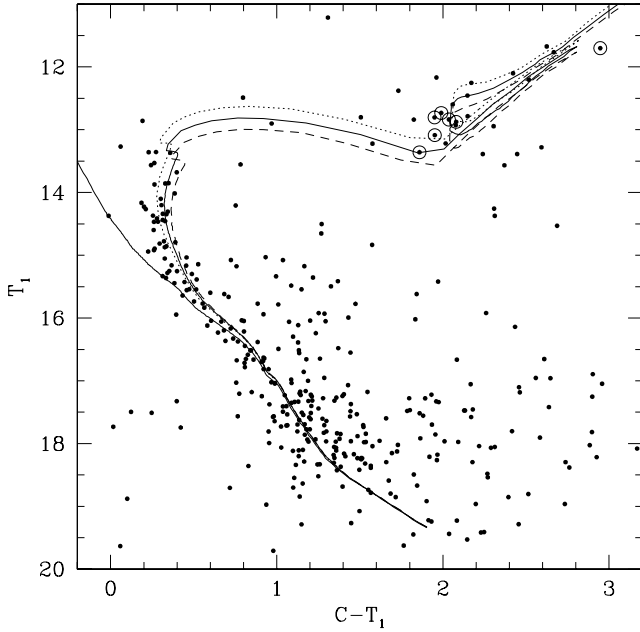


Fig. 8. $(T_1, C - T_1)$ colour-magnitude diagram for stars in NGC 2324. Isochrones from Lejeune & Schaerer (2001) of $\log t = 8.60, 8.65$ and 8.70 , computed taking into account overshooting, are overlotted with dotted, solid and short-dashed lines, respectively.

we derive $E(B - V) = 0.20 \pm 0.05$ and $d = (4.0 \pm 0.5)$ kpc for the cluster. Figure 8 shows the isochrone for the adopted cluster age and metallicity (solid line) and two additional isochrones of $\log t = 8.60$ and 8.70 with dotted and short dashed lines, respectively, for comparison purposes. The ZAMS and the red giant members of Mermilliod et al. (2001) are also drawn with the same symbols as in Fig. 7. Note that the RGC appears now better fitted by the theoretical isochrones in comparison to those of Fig. 7. The fundamental parameters estimated from both photometries proved to be in very good agreement. Therefore, we adopted those coming from the *VI* data for the subsequent analysis.

4.1. Metal content

As it has already been described in Sect. 1, the various determinations of metallicity based on photometric and/or spectroscopic data of red giants in NGC 2324 yield very discrepant values. In particular, Geisler et al. (1992, hereafter GCM92) derived an unexpectedly low value ($[\text{Fe}/\text{H}] = -1.01 \pm 0.27$) from very accurate Washington photoelectric data of 14 red giant stars. Considering that the five abundance indices defined in this system are very sensitive to reddening (Geisler et al. 1991, hereafter GCM91), it is evident that the remarkably low metal abundance derived by GCM92 is mainly due to the fact that they adopted for the cluster $E(B - V) = 0.11$, a value which is considerably lower than the one found in the present work. Taking into account the fact that Mermilliod et al. (2001) have unambiguously identified 5 red giants (single stars) with constant radial velocity (Cuffey's star numbers 19, 67, 136, 161 and 215), we decided to use the $E(B - V)$ reddening value here derived, the original photoelectric data obtained by GCM92

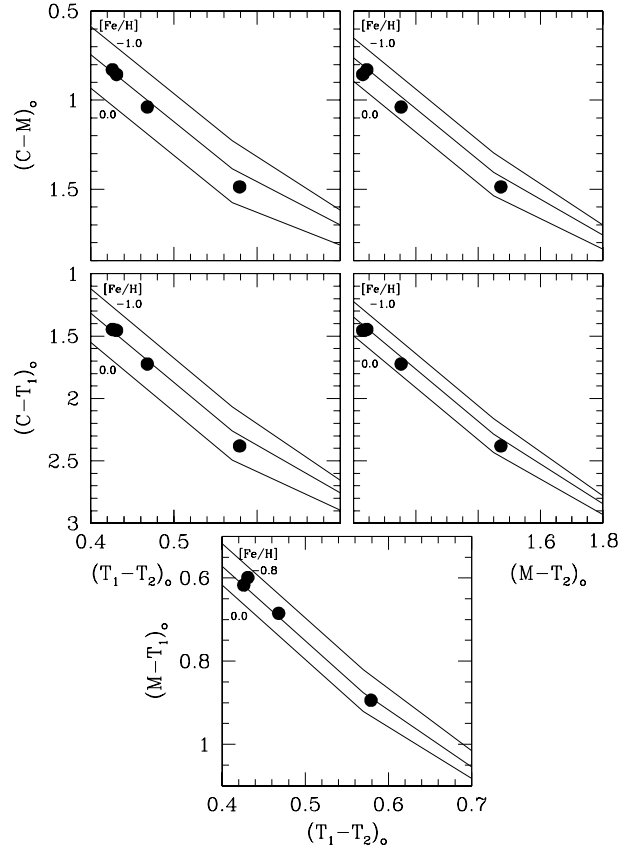


Fig. 9. Unreddened Washington colour-colour diagrams for 4 red cluster giants confirmed from Coravel radial velocity data. Isoabundance relations from Geisler et al. (1991) for 0.5 dex intervals from $[\text{Fe}/\text{H}] = -1.0$ to 0.0 are shown, except for the $(M - T_1)_0/(T_1 - T_2)_0$ diagram wherein isoabundance relations for 0.4 dex intervals from -0.8 to 0.0 are given.

and the iterative method described by GCM91 to redetermine the cluster metal content.

The observed Washington colours were firstly corrected for reddening using the following colour excess ratios given by GCM91: $E(C - M)/E(B - V) = 1.066$, $E(M - T_1)/E(B - V) = 0.90$, $E(T_1 - T_2)/E(B - V) = 0.692$, $E(C - T_1)/E(B - V) = 1.966$ and $E(M - T_2)/E(B - V) = 1.592$. Then, we used the reddening-corrected isoabundance relations between $C - M$ and $T_1 - T_2$ indices, $M - T_1$ and $T_1 - T_2$, $C - T_1$ and $T_1 - T_2$, $C - M$ and $M - T_2$, and $C - T_1$ and $M - T_2$. Figure 9 shows the five two-colour relations for 4 of the above 5 confirmed red cluster giants, since star 19 with $(T_1 - T_2)_0 = 0.366$ and $(M - T_2)_0 = 0.943$, falls outside the range of the GCM91 calibrations. Note that the four confirmed red cluster giants lie between the isoabundance lines corresponding to $[\text{Fe}/\text{H}] = 0.0$ and -0.5 in practically all cases in Fig. 9.

For each star we computed the metallicity sensitive Δ' value for each index as defined in GCM91. Following their nomenclature, we denote $\Delta'(C - M)_{T_1 - T_2}$ as Δ'_1 , $\Delta'(M - T_1)_{T_1 - T_2}$ as Δ'_2 , $\Delta'(C - T_1)_{T_1 - T_2}$ as Δ'_3 , $\Delta'(C - M)_{M - T_2}$ as Δ'_4 and $\Delta'(C - T_1)_{M - T_2}$ as Δ'_5 . The resulting mean values and standard deviations from the 4 confirmed red cluster giants are: $\Delta'_1 = -0.131 \pm 0.023$, $\Delta'_2 = -0.042 \pm 0.007$, $\Delta'_3 = -0.158 \pm 0.016$, $\Delta'_4 = -0.070 \pm 0.012$, and $\Delta'_5 = -0.088 \pm 0.013$. These values practically do

not change if the 3 spectroscopic binaries (Cuffey's star numbers 91, 118 and 134) are included. Using the abundance calibrations of GCM91, the above mean indices yield: $[\text{Fe}/\text{H}]_1 = -0.33 \pm 0.07$, $[\text{Fe}/\text{H}]_2 = -0.37 \pm 0.06$, $[\text{Fe}/\text{H}]_3 = -0.33 \pm 0.04$, $[\text{Fe}/\text{H}]_4 = -0.25 \pm 0.05$ and $[\text{Fe}/\text{H}]_5 = -0.28 \pm 0.05$. We finally adopted for NGC 2324 the average of the five Washington abundance estimates: $[\text{Fe}/\text{H}] = -0.31 \pm 0.04$ (s.d.), which is in reasonable agreement with the metallicity value derived from the isochrone fitting. Note that if the stars 191 and 801 of their list were omitted, the metallicity adopted by Friel et al. (2002) for NGC 2324 ($[\text{Fe}/\text{H}] = -0.15 \pm 0.16$) would result in a lower value ($[\text{Fe}/\text{H}] = -0.23 \pm 0.06$).

5. Discussion

As mentioned in Sect. 1, there are several works in the literature dedicated to study NGC 2324. Unfortunately, however, many of them are based on photographic data and their results do not seem to be in close agreement. The most recent overall parameter determination was carried out by Kyeong et al. (2001, hereafter KBS01) from CCD *UBVI* photometry. Using a scale of $0''.6 \text{ pix}^{-1}$ larger than ours, KBS01 derived for the cluster a $E(B - V)$ colour excess of 0.17 ± 0.12 , a $V - M_V$ apparent modulus of 13.6 ± 0.1 , a metallicity of $[\text{Fe}/\text{H}] = -0.32$ and an age of 630 Myr. Their cluster reddening, distance and metallicity values are nearly similar to the present estimates within the quoted uncertainties. However, the age estimated by KBS01 appears to be 40 per cent older than our value. Looking at KBS01's Fig. 4, we note that the upper cluster MS ends at $V \approx 14.0$, while in our photometry it reaches slightly above $V = 13.5$ (see Fig. 7). The RGC of KSB01 also appears to be less populated than our RGC. We believe that due to the limiting brighter magnitude observed by KBS01, they chose an older isochrone to properly adjust the cluster turn-off, which in turn translates into a theoretical RGC fainter than the observed one. We attribute this magnitude cut in their CMDs to their having employed relatively long exposures (our exposures are 5–10 times shorter with a slightly smaller telescope aperture) which led to the saturation of the brightest stars. However, the finding chart of their Fig. 1 surprisingly shows some very bright stars which we have not been able to identify in our Fig. 1. Our impression is that the finding chart published by KBS01 definitely does not correspond to that of the cluster.

The method used by Mermilliod et al. (2001) to estimate the cluster properties consists in looking for the isochrone which best reproduces the morphology of the red giant pattern, defined by stars unambiguously confirmed as members from accurate radial velocity measures. Thus, they derived $E(B - V) = 0.02$, $V - M_V = 12.95$, $[\text{Fe}/\text{H}] = 0.02$, and $\log t = 8.90$ (~ 800 Myr). Note that the method uses as reference the magnitude and colour of the RGC. This is the reason why their colour excess, for example, is nearly equal to the $\Delta(V - I)$ colour offset we found for the theoretical RGC, if compared to the observed one (see Sect. 4). The fact of considering as reference the RGC in the fitting procedure could also explain the large difference in the cluster age found by Mermilliod et al. (2001).

With the aim of locating NGC 2324 in the general framework of the structure and chemical evolution of the Galactic

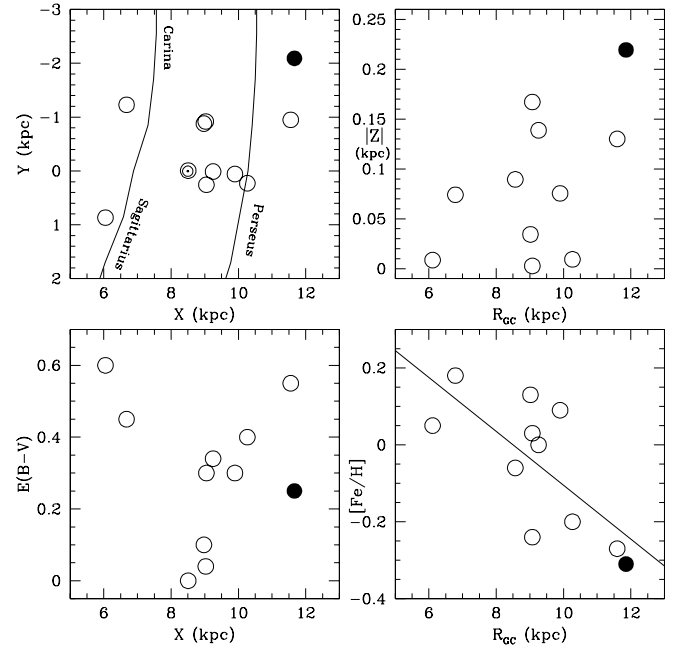


Fig. 10. Relationships between the different Galactic coordinates, the reddening and the metallicity of open clusters of Table 4. Open circles and the filled circle represent clusters of Table 4 and NGC 2324, respectively. The Carina-Sagittarius and Perseus spiral arms and the position of the Sun are indicated in the upper left-hand panel. The solid line in the lower right-hand panel represents an abundance gradient of $-0.07 \text{ dex kpc}^{-1}$. See Sect. 5 for details.

disc, we searched through the WEBDA open cluster Data Base (see, <http://obswww.unige.ch/webda/>) and in the available literature for objects with ages between 400 and 500 Myrs. Since WEBDA is a compilation of open cluster data from various sources and Sarajedini (1999) showed that WEBDA ages are younger by $\log t = 0.191$ than his age scale, we also searched through other recent compilations and catalogues of open clusters (Piatti et al. 1995; Twarog et al. 1997; Chen et al. 2003, among others). We found a sample of 10 open clusters within the desired age range which have well-known fundamental parameters. Table 4 lists their Galactic coordinates, distances, reddenings, ages and metallicities, together with the references from which all these quantities were taken. Clusters with no reliable fundamental parameters were not included in Table 4. We computed the Galactic coordinates X , Y and Z and the Galactocentric distances R_{GC} for all the clusters from their Galactic coordinates (l , b) and distances from the Sun, assuming the Sun's distance from the centre of the Galaxy to be 8.5 kpc. The computed values are listed in the four last columns of Table 4.

The upper left-hand panel of Fig. 10 shows the projected spatial distribution of the 10 selected clusters onto the Galactic plane. We have drawn the selected clusters and NGC 2324 with open circles and a filled circle, respectively, and we have marked the position of the Sun as well. The curves schematically represent the spiral arms of Carina-Sagittarius and Perseus as mapped by H II regions and the dust (Drimmel & Spergel 2001). The clusters are distributed over a relatively extended portion of the observationally reachable Galactic

Table 4. Fundamental parameters of selected open clusters.

Star cluster	l ($^{\circ}$)	b ($^{\circ}$)	d (kpc)	$E(B - V)$ (mag)	Age (Gyr)	[Fe/H]	References	X (kpc)	Y (kpc)	Z (kpc)	R_{GC} (kpc)
NGC 1342	154.99	-15.38	0.63	0.30	0.50	-0.24	1, 2	9.05	0.26	-0.17	9.08
NGC 1758	179.15	-10.52	0.76	0.34	0.40	0.00	5	9.25	0.01	-0.14	9.26
NGC 1907	172.62	+00.30	1.78	0.40	0.40	-0.20	12, 13	10.27	0.23	0.01	10.27
NGC 2099	177.65	+03.09	1.40	0.30	0.40	0.09	4, 11	9.90	0.06	0.07	9.90
NGC 2194	197.26	-02.33	3.20	0.55	0.40	-0.27	10	11.55	-0.95	-0.13	11.59
NGC 2324	213.44	+03.32	3.80	0.25	0.44	-0.31	14	11.66	-2.09	0.22	11.86
NGC 2447	240.07	+00.15	1.06	0.04	0.45	0.03	3	9.03	-0.92	0.00	9.08
NGC 2482	241.63	+01.97	1.00	0.10	0.40	0.13	2, 4	8.98	-0.88	0.03	9.02
NGC 5999	326.02	-01.93	2.20	0.45	0.40	0.18	6, 7	6.68	-1.23	-0.07	6.79
NGC 6631	19.47	-00.19	2.60	0.60	0.40	0.05	8	6.05	0.87	-0.01	6.11
Melotte 111	221.20	+84.01	0.09	0.00	0.50	-0.06	9	8.51	-0.01	0.09	8.57

REFERENCES: (1) Jennens & Helfer (1975); (2) Piatti et al. (1995); (3) Hamdani et al. (2000); (4) Twarog et al. (1997); (5) Galadi-Enrquez et al. (1998); (6) Piatti et al. (1999); (7) Santos & Bica (1993); (8) Sagar et al. (2001); (9) Odenkirchen et al. (1998); (10) Paper I; (11) Nilakshi & Sagar (2002); (12) Strobel (1991); (13) Subramaniam & Sagar (1999); (14) this study.

disc. Piatti et al. (1995) computed galactic orbits for 19 open clusters, two of which are included in Table 4 (NGC 1342 and NGC 2099), and calculated their perigalactic (R_p) and apogalactic (R_a) distances, as well as the maximum values of the heights out of the Galactic plane ($|Z_{max}|$). They obtained $(R_p, R_a, |Z_{max}|) = (5.71, 9.01, 0.75)$ kpc and $(7.02, 9.85, 0.19)$ kpc for NGC 1342 and NGC 2099, using as current positions $(R_{GC}, Z) = (8.99, -0.15)$ kpc and $(9.85, 0.07)$ kpc, respectively. As can be inferred, there is not any evidence that the clusters were mainly formed either near the present positions 400–500 Myr ago, or in the spiral arms. Note that Piatti et al. (1995) found that the difference between the perigalactic and apogalactic distances for their sample of 19 open clusters is only 3 kpc.

NGC 2324 is not only the farthest cluster from the Sun and from the Galactic centre of the selected sample (upper left-hand panel), but also the most distant one from the Galactic plane (upper right-hand panel). According to its height Z out of the Galactic plane (220 pc), NGC 2324 would be located within the thin disc, which allows us to indistinctly use $X \equiv R_{GC}$ (see also Table 4) for all the clusters in the subsequent analysis. The metallicity and the Galactocentric distance derived for NGC 2324 are in excellent accordance with the generally accepted radial abundance gradient of -0.07 kpc^{-1} for the disc of the Galaxy (see, e.g., Piatti et al. 1995; Friel et al. 2002; Chen et al. 2003). The straight solid line in the lower right-hand panel of Fig. 10 shows the aforementioned abundance gradient. Given the fact that the remaining clusters of the sample also follow a similar trend, and since that size of the gradient has been documented for the earliest epoch of the Galactic disc (Piatti et al. 1995; Friel et al. 2002; Hou et al. 2002), we conclude that the present gradient is very close to the paleogradient one, namely, the gradient in metallicity of the gas out of which the clusters have been formed. Notice that the abundance gradient traced by the selected clusters is affected neither by their ages

(they are practically coeval) nor by their distribution above or below the Galactic plane (they are in the thin disc).

The lower left-hand panel of Fig. 10 shows the relationship between the $E(B - V)$ colour excess and the Galactic coordinate X (or equivalently R_{GC}). Two clusters, NGC 5999 and NGC 6631, are located behind the Carina-Sagittarius arm when looking at them from the Sun (see the upper left-hand panel). Their relatively high reddenings could be caused by the presence of the spiral arms, since these two clusters are located at low Galactic latitudes. Similarly, NGC 2194 and NGC 2324 are placed beyond the Perseus arm, but only NGC 2194 has a reddening comparable to those of NGC 5999 and NGC 6631. NGC 2324 is farther from the Sun than NGC 2194 and is also at a larger height Z from the Galactic plane, but its reddening is nearly half of the NGC 2194’s $E(B - V)$ colour excess. At this point, it is difficult to assert whether the lower reddening of NGC 2194 is owing to its larger separation from the Galactic plane, to the known patchy distribution of the interstellar matter in the Galactic disk, or to both effects combined.

6. Conclusions

New CCD observations in the Johnson V , Kron-Cousins I and the Washington system C and T_1 passbands have been used to build CMDs reaching down to $V \sim 20$ and $T_1 \sim 18.5$ for NGC 2324, a relatively young open cluster located near the Galactic anticentre direction. The analysis of the photometric data leads to the following main conclusions:

- (i) Since the field star composition varies across the observed sky area, we used the innermost $r < 400$ pixels CMDs as representative of the cluster ($V, V - I$) and ($T_1, C - T_1$) diagrams. Hence, we derived from them the basic cluster parameters. These CMDs reveal a group of RGC stars at $(V, V - I) \approx (13.3, 1.15)$ and $(T_1, C - T_1) \approx (12.8, 2.0)$,

respectively. An examination of the observed CMDs shows that NGC 2324 is a moderated reddened object, slightly younger than the Hyades. The comparison of the cluster CMDs with theoretical isochrones of the Geneva group suggests that the cluster has a metallicity lower than the solar one. For $Z = 0.008$, equivalent to $[\text{Fe}/\text{H}] = -0.40$, the best-fitting isochrones implies $E(V - I) = 0.33 \pm 0.07$, $V - M_V = 13.70 \pm 0.15$, $E(C - T_1) = 0.40 \pm 0.10$, $T_1 - M_{T_1} = 13.65 \pm 0.15$ and an age of 440 Myr. NGC 2324 is then located at a distance of 3.8 kpc from the Sun, its mean $E(B - V)$ colour excess being 0.25 ± 0.05 .

- (ii) A cluster angular radius of 5.3 ± 0.3 , equivalent to (5.9 ± 0.3) pc, was estimated from star counts performed within and outside the cluster area.
- (iii) Using the method described by Geisler et al. (1991), a cluster metal abundance $[\text{Fe}/\text{H}] = -0.31 \pm 0.04$ relative to the Sun was derived from Washington photometric data of 4 red giants (single stars), which were unambiguously identified as cluster members from Coravel radial velocities (Mermilliod et al. 2001). This value is in reasonable agreement with that derived from the best isochrone fitting. Therefore, NGC 2324 is found to be a relatively young, metal-poor and distant open cluster located beyond the Perseus spiral arm.
- (iv) A comparison of NGC 2324 with a sample of well-known open clusters of nearly the same age confirms the existence of a radial abundance gradient of -0.07 dex kpc^{-1} in the Galactic disc.

Acknowledgements. We are gratefully indebted to the CTIO staff for their hospitality and support during the observing run. We also thank referee J.-C. Mermilliod for his valuable comments. This work was partially supported by the Argentinian institutions CONICET, SECYT (Universidad Nacional de Córdoba), Agencia Córdoba Ciencia and Agencia Nacional de Promoción Científica y Tecnológica (ANPCyT). This work is based on observations made at Cerro Tololo Inter-American Observatory, which is operated by AURA, Inc., under cooperative agreement with the NSF.

References

- Alter, G., Ruprecht, J., & Vanisek, J. 1970, Catalogue of Star Clusters and Associations, Akademiai Kiado, Budapest
- Barkhatova, K. A. 1963, Sb. Ural Univ., 1, 3
- Becker, W. 1960, Z. Astrophys., 51, 45
- Becker, W., & Fenkart, R. 1971, A&AS, 4, 241
- Becker, W., Svolopoulos, S. N., & Fang, C. 1976, Kataloge photographischer und photoelektrischer Helligkeiten von 25 galaktischen Sternhaufen im RGU- und UcbV System (Basel)
- Bertelli, G., Bressan, A., Chiosi, C., Fagoto, F., & Nasi, F. 1994, A&A, 106, 275
- Canterna, R. 1976, AJ, 81, 228
- Chen, L., Hou, J. L., & Wang, J. J. 2003, AJ, 125, 1397
- Clariá, J. J., Mermilliod, J.-C., & Piatti, A. E. 1999, A&AS, 134, 301
- Clariá, J. J., Mermilliod, J.-C., Piatti, A. E., & Minniti, D. 1994, A&AS, 107, 39
- Collinder, P. 1931, Medd. Lunds. Astron. Obs., 2
- Cuffey, J. 1941, ApJ, 94, 55
- Drimmel, R., & Spergel, D. N. 2001, ApJ, 556, 181
- Dutra, C. M., & Bica, E. 2000, A&A, 359, 347
- Friel, E. D. 1995, ARA&A, 33, 381
- Friel, E. D., Janes, K. A., Tavarez, M., et al. 2002, AJ, 124, 2693
- Galadi-Enríquez, D., Jordi, C., & Trullols, E. 1998, A&A, 337, 125
- Geisler, D. 1996, AJ, 111, 480
- Geisler, D., Clariá, J. J., & Minniti, D. 1991, AJ, 102, 1836 (GCM91)
- Geisler, D., Clariá, J. J., & Minniti, D. 1992, AJ, 104, 1892 (GCM92)
- Geisler, D., Lee, M. G., & Kim, E. 1996, AJ, 111, 1529
- Geisler, D., Piatti, A. E., Bica, E., & Clariá, J. J. 2003, MNRAS, 341, 771
- Gratton, R. 2000, in Stellar Clusters and Associations: Convection, Rotation, and Dynamics, ed. R. Pallavicini, G. Micela, & S. Sciortino (San Francisco: ASP), ASP Conf. Ser., 198, 225
- Hamdani, S., North, P., Mowlavi, N., Raboud, D., & Mermilliod, J.-C. 2000, A&A, 360, 509
- Hoag, A. A., Johnson, H. L., Iriarte, B., et al. 1961, Publ. US Naval Obs., Second Ser., XVII, VII, 347
- Hou, J.-L., Chang, R.-X., & Chen, L. 2002, ChJ&A, 2, 17
- Janes, K. A. 1979, ApJS, 39, 135
- Janes, K. A., & Phelps, R. L. 1994, AJ, 108, 1773
- Jennens, P. A., & Helfer, H. L. 1975, MNRAS, 172, 681
- Kyeong, J.-M., Byun, Y.-I., & Sung, E.-Ch. 2001, JKAS, 34, 143
- Landolt, A. U. 1992, AJ, 104, 340
- Lejeune, T., & Schaerer, D. 2001, A&A, 366, 538
- Loktin, A., Gerasimenko, T., & Malisheva, L. 2001, A&A Trans., 20, 605
- Loktin, A., & Matkin, N. V. 1994, A&A Trans., 4, 153
- Lyngå, G. 1987, Catalogue of Open Cluster Data, Strasbourg, Centre de Données Stellaires
- Mermilliod, J.-C., Clariá, J. J., Andersen, J., Piatti, A. E., & Mayor, M. 2001, A&A, 375, 30
- Nilakshi, D., & Sagar, R. 2002, A&A, 381, 65
- Odenkirchen, M., Soubiran, C., & Colin, J. 1998, New Astron., 3, 583
- Perryman, M. A. C., Brown, A. G. A., Lebreton, Y., et al. 1998, A&A, 331, 81
- Phelps, R. L., Janes, K. A., & Montgomery, K. A. 1994, AJ, 107, 1079
- Piatti, A. E., Clariá, J. J., & Abadi, M. G. 1995, AJ, 110, 2813
- Piatti, A. E., Clariá, J. J., & Ahumada, A. V. 2003a, MNRAS, 340, 1249 (Paper I)
- Piatti, A. E., Clariá, J. J., & Ahumada, A. V. 2003b, MNRAS, 346, 390
- Piatti, A. E., Clariá, J. J., & Ahumada, A. V. 2004, MNRAS, in press
- Piatti, A. E., Clariá, J. J., & Bica, E. 1998, ApJS, 116, 263
- Piatti, A. E., Clariá, J. J., & Bica, E. 1999, MNRAS, 303, 65
- Rahim, M. A., & Hassan, S. M. 1967, Helwan Obs. Bull., No. 7
- Ruprecht, J. 1966, Bull. Astron. Inst. Czech., 17, 33
- Sagar, R., Naidu, B. N., & Mohan, V. 2001, Bull. Astron. Soc. India, 29, 519
- Santos, J. F. C. Jr., & Bica, E. 1993, MNRAS, 260, 915
- Sarajedini, A. 1999, AJ, 118, 2321
- Stetson, P. B. 1987, PASP, 99, 191
- Strobel, A. 1991, ApJ, 376, 204
- Subramaniam, A., & Sagar, R. 1999, AJ, 117, 937
- Twarog, B. A., Ashman, K. M., & Anthony-Twarog, B. J. 1997, AJ, 114, 2556